Received: 6 May 2021 | Revised: 19 October 2021 | Accepted: 6 December 2021

DOI: 10.1111/psyp.13999

PSYCHOPHYSIOLOGY SPR WILEY

ORIGINAL ARTICLE

Are alpha and beta oscillations spatially dissociated over the cortex in context-driven spoken-word production?

Yang Cao[1] | Robert Oostenveld[2,3] | Phillip M. Alday[4] | Vitória Piai[1,5]

[1]Donders Centre for Cognition, Radboud University, Nijmegen, The Netherlands

[2]Donders Centre for Cognitive Neuroimaging, Radboud University, Nijmegen, The Netherlands

[3]NatMEG, Karolinska Institutet, Stockholm, Sweden

[4]Max-Planck-Institute for Psycholinguistics, Nijmegen, The Netherlands

[5]Donders Centre for Medical Neuroscience, Department of Medical Psychology, Radboud University Medical Center, Nijmegen, The Netherlands

Correspondence
Yang Cao, Donders Institute for Brain, Cognition, and Behaviour, Donders Centre for Cognition, Radboud University, Montessorilaan 3, 6525 HR Nijmegen, The Netherlands.
Email: yang.cao@donders.ru.nl

Funding information
This research was supported by China Scholarship Council (CSC) scholarship (No.202007720076 to Y.C.) and grants from the Netherlands Organization for Scientific Research (446-13-009 to V.P. and 400-09-138 to Ardi Roelofs)

Abstract

Decreases in oscillatory alpha- and beta-band power have been consistently found in spoken-word production. These have been linked to both motor preparation and conceptual-lexical retrieval processes. However, the observed power decreases have a broad frequency range that spans two "classic" (sensorimotor) bands: alpha and beta. It remains unclear whether alpha- and beta-band power decreases contribute independently when a spoken word is planned. Using a re-analysis of existing magnetoencephalography data, we probed whether the effects in alpha and beta bands are spatially distinct. Participants read a sentence that was either constraining or non-constraining toward the final word, which was presented as a picture. In separate blocks participants had to name the picture or score its predictability via button press. Irregular-resampling auto-spectral analysis (IRASA) was used to isolate the oscillatory activity in the alpha and beta bands from the background 1-over-f spectrum. The sources of alpha- and beta-band oscillations were localized based on the participants' individualized peak frequencies. For both tasks, alpha- and beta-power decreases overlapped in left posterior temporal and inferior parietal cortex, regions that have previously been associated with conceptual and lexical processes. The spatial distributions of the alpha and beta power effects were spatially similar in these regions to the extent we could assess it. By contrast, for left frontal regions, the spatial distributions differed between alpha and beta effects. Our results suggest that for conceptual-lexical retrieval, alpha and beta oscillations do not dissociate spatially and, thus, are distinct from the classical sensorimotor alpha and beta oscillations.

KEYWORDS

anterior temporal lobe, context, picture naming, prediction, word production

1 | INTRODUCTION

Brain oscillations are produced by coordinated electrophysiological activity of large groups of neurons and can be studied with electroencephalography (EEG) and magnetoencephalography (MEG) (Buzsáki & Draguhn, 2004). The German neurologist Berger, when first recording the electroencephalogram on the human scalp, found rhythmic voltage fluctuations at about 10 Hz on a person's posterior scalp when the eyes were closed, which changed

into fluctuations of higher frequency when the eyes were open. In 1929, he reported these findings using the terms "alpha" and "beta" waves (Karakaş & Barry, 2017). Later, two other components were found to fluctuate in the same frequency range of 7–13 Hz: the mu rhythm in motor areas (Pfurtscheller et al., 1997) and the tau rhythm in the auditory temporal lobe (Lehtelä et al., 1997; Niedermeyer, 1993). Today, the term "alpha" is typically used to indicate the electrophysiological activity in the 8–12 Hz range, and "beta" in the 13–30 Hz range.

Neural oscillations have been argued to provide an avenue to understand how general neuronal computational principles support language (Friederici & Singer, 2015; Piai & Zheng, 2019). In other cognitive domains, different frequency bands have been associated with specific functions, such as power increases in the theta (4–7 Hz) and decreases in the alpha and beta bands with successful memory encoding and retrieval (Hanslmayr et al., 2012; Nyhus & Curran, 2010), and alpha and beta power decreases with motor preparation and execution (Cheyne, 2013). However, it remains unclear how the different frequency bands relate to specific processes employed in language processing.

When producing words, speakers go from having a concept they want to convey, to translating it into a verbal message, and finally into motor commands (Dell et al., 1997; Levelt et al., 1999). These steps are achieved through both memory (i.e., retrieval of conceptual, lexical, and phonological information from long-term memory) and motor processes (i.e., preparation and execution of an articulatory program). Studies have suggested a functional relationship between neural oscillations in the alpha and beta bands and language production. Alpha- and beta-band power decreases were initially linked to the motor cortex (Crone & Hao, 2002; Salmelin & Sams, 2002; Salmelin et al., 2000), but later studies indicated they could also index word-retrieval processes (Piai et al., 2014, 2015, 2020). However, these past findings comprise two "classical bands" of (sensorimotor) rhythms, alpha and beta, with possibly distinct roles in human cognition.

The alpha and beta rhythms are adjacent in the frequency spectrum and have often been found hand in hand in the motor domain over sensorimotor regions (e.g., Jurkiewicz et al., 2006; De Lange et al., 2008), in the memory domain (for a review, see Hanslmayr et al., 2012), and in the language domain (Piai et al., 2014, 2015, 2017, 2018; Wang et al., 2012, 2017). In the motor domain, the two bands may show partial overlap in spatial distribution (Szurhaj et al., 2003; Yuan et al., 2010), and temporally correlated power envelopes (De Lange et al., 2008; Tiihonen et al., 1989, see also Sederberg et al., 2003 for a high degree of overlap between sites in the memory domain). However, other studies in the motor domain have demonstrated that alpha and beta have different features. For example, beta oscillations, and to a lesser extent alpha, are coherent with the electromyogram of muscles (Brown, 2000; Mima & Hallett, 1999) and somatotopically organized in an effector-specific way (Crone et al., 1998; Salmelin et al., 1995). Recent studies have further suggested that sensorimotor alpha and beta oscillations have both anatomical and functional specificities. For instance, a recent study using intracranial EEG recordings indicated that alpha and beta have different anatomical distributions and travel along opposite directions across the sensorimotor cortex (Stolk et al., 2019). Here, alpha was proposed to support the disengagement of the task-irrelevant somatosensory cortical regions ipsilateral to the selected arm. By contrast, beta was argued to mediate the disinhibition of neuronal populations involved in the computations of movement parameters of the motor cortex contralateral to the selected arm (Brinkman et al., 2014; Stolk et al., 2019). Thus, alpha and beta power decreases support movement with different functional mechanisms (Brinkman et al., 2014; Stolk et al., 2019), and this notion has been supported by causal evidence using transcranial alternating current stimulation (Brinkman et al., 2016; Wach et al., 2013). Importantly, however, none of the previous studies on oscillations related to retrieval in language production have addressed the question whether the power decreases within the broad frequency range of the classical alpha and beta bands are brought about by a unitary or two distinct mechanisms.

Piai and colleagues (Klaus et al., 2020; Piai et al., 2015, 2017, 2020, 2014, 2018; Roos & Piai, 2020) employed a picture-naming task in which the pictures that were to be named (e.g., "key") are preceded by either a constraining (e.g., "He locked the door with the ...") or non-constraining (e.g., "She walked in here with the ...") lead-in sentence context. The pictures are named faster following the constraining contexts relative to non-constraining ones. Prior to picture onset, EEG and MEG alpha- and beta-band power decreases have been repeatedly observed for constraining relative to non-constraining contexts, accompanying the behavioral facilitation. These power decreases localize to the left angular and supramarginal gyri, left anterior and posterior temporal cortex (associated with retrieval of linguistic information), and to areas associated with motor preparation in language production (Piai et al., 2015; Roos & Piai, 2020). Word planning at the conceptual, the lexical, and even the phonological level can already start *before* the picture onset with a constraining context, whereas when preceded by a non-constraining context, the conceptual, lexical, and phonological information can only be retrieved from memory *after* the presentation of the picture. The differences in alpha- and beta-band power between the context conditions pre-picture onset

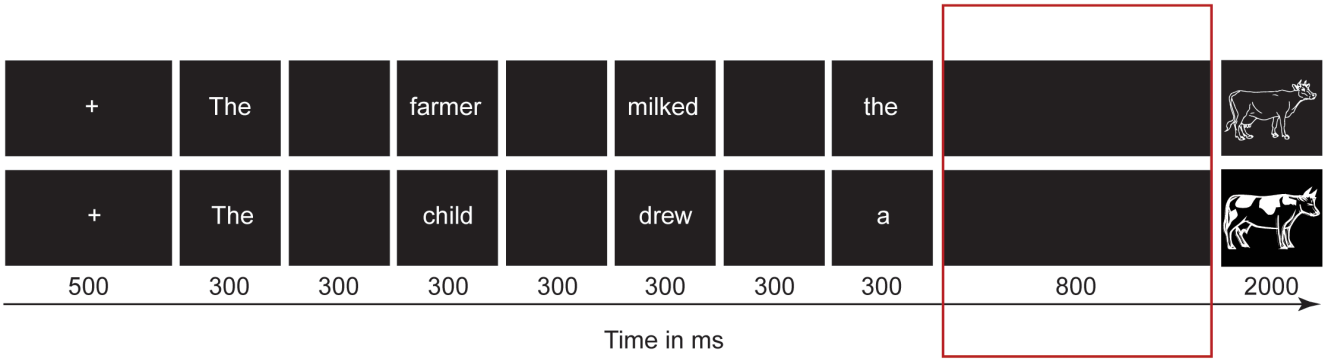

FIGURE 1 An example of trials for the target picture "cow" in the constraining (upper) and non-constraining (lower) conditions. Presentation duration of each event in the trial is given below the boxes. The 800 ms black screen before the picture onset marked in red was the time window of interest for analysis

were, thus, reasoned to reflect the differential engagement of the language production system, and in particular, retrieval of information from memory and motor preparation of a spoken word (Piai et al., 2015).

Despite the robust evidence for alpha- and beta-band power decreases supporting word production, it remains an open question whether they support a single unitary operation or contribute independently when a spoken word is produced. To address this question, we reanalysed existing MEG data (Piai et al., 2015) to assess the spatial specificity of the alpha- and beta-band power decreases in context-driven spoken word production. Participants overtly named a picture (Naming task) or pressed a button to score its predictability (Judgment task) after reading the sentences. The two tasks were split over separate experimental blocks. The Judgment task, in which participants pressed the button with their left hand to indicate whether the picture was expected, served as a control task to index attentional effects, conceptual preparation, which were similar to the Naming task, and general motor preparation. For both tasks, we examined the spatial distribution of the context effects, that is, the contrasts between the constraining vs non-constraining conditions, in both oscillatory bands separately. According to a recent proposal, certain methodological considerations are needed for the analysis of neural oscillations (Donoghue et al., 2021). In particular, the presence of oscillations should be verified, the oscillatory bands should be validated, and concurrent non-oscillatory activity should be accounted for. To take these considerations into account, and better isolate the alpha and beta bands and identify the peak frequencies for each individual participant, we used an irregular-resampling autospectral analysis (IRASA, Wen & Liu, 2016). IRASA allows distinguishing rhythmic activity from the concurrent power-spectral $1/f$ modulation. Broadband arrhythmic activity, which has a $1/f$ like spectrum, co-occurs with rhythmic activity in the brain. Traditional narrowband analyses on pre-specified frequency bands (e.g., alpha as 8–12 Hz) do not account for this co-occurrence (e.g., Donoghue et al., 2020). As the exact slope of the $1/f$ component differs between individuals, the contribution of $1/f$ over alpha and beta power will also differ, thus confounding alpha- and beta-band results. The IRASA procedure, which improves the spectral precision of oscillatory peak frequencies by controlling for effects of task-related modulations in the $1/f$ spectral component (He, 2014), serves to reduce/remove this confound, thus providing an estimate of alpha- and beta-band power decoupled from interindividual differences in arrhythmic activity. We assessed whether the previously observed power decreases associated with the context effect based on narrowband approaches reflect oscillatory activity. We then source localized the context effects in both the Naming and Judgment tasks using individualized peaks for alpha and beta, instead of using canonical alpha and beta bands. To compare the spatial distribution of the source-reconstructed alpha and beta effects in frontal and temporo-parietal cortices, we used both correlation analyses and the earth mover's distance (EMD) measure (Rubner et al., 2000), which provides a measure of the distance between two distributions.

2 | METHOD

Here we reanalyzed the published data of Piai et al. (2015) to examine the spatial dissociation of alpha and beta oscillations. In Piai et al., participants read the constraining or non-constraining sentence context with the last word of the sentence presented as a picture (example, see Figure 1). Participants were instructed to perform two tasks in different experimental blocks: Picture Naming (i.e., overtly produce the

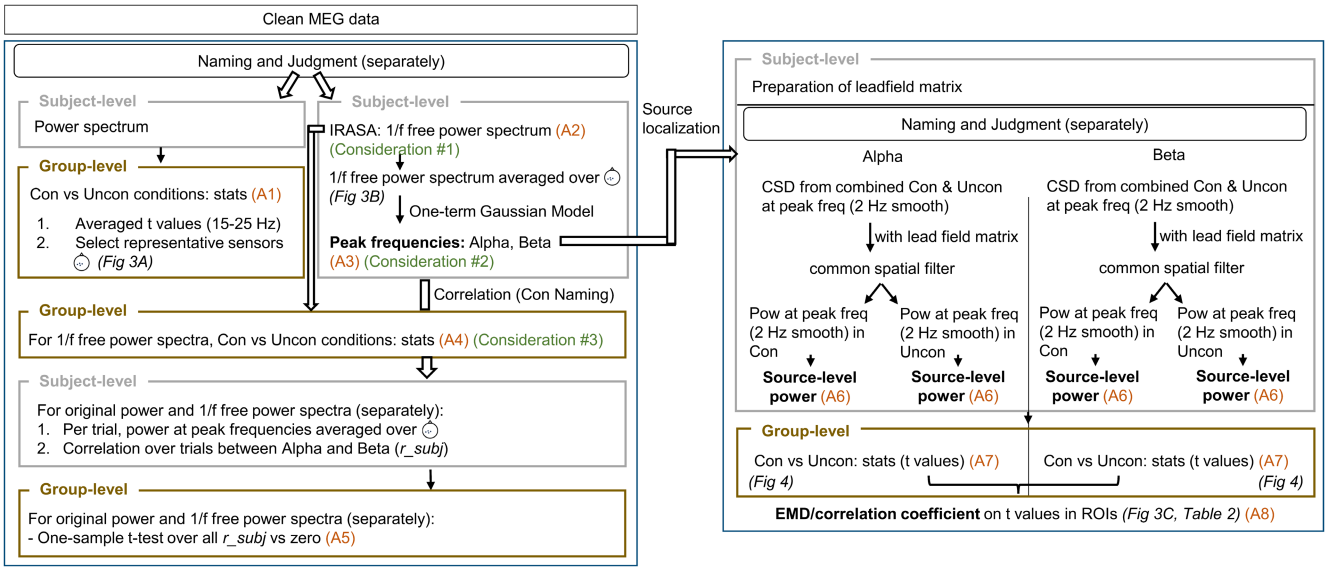

FIGURE 2 Data processing flowchart. The left-hand side indicates the sensor-level analyses and the right-hand side the source-level analyses. The level of processing (i.e., participant or group level) is indicated in the top left corner of the boxes, with the group-level analysis marked in brown. The connection between different analysis steps in the figure and in the text is indicated by A1–A8. Con, constraining; CSD, cross-spectral density; freq, frequency; pow, power; ROI, region of interest; Uncon, non-constraining

picture's name) and Picture Judgment (i.e., a left-hand button press to indicate whether the picture was expected). The order of Naming and Judgment tasks was counterbalanced across participants. For each task, each context condition (constraining/non-constraining) consisted of 84 trials (see Piai et al., 2015, for details on materials and design). From the 19 participants of the Piai et al. study, two were rejected due to excessive blinking. Further, for all source-level analyses, data from three additional participants were excluded from further analysis because we did not have structural magnetic resonance imaging (MRI) data for those participants, and one additional participant was excluded because of having two peaks in the alpha range (see Sensor-level analysis below). This left us with data from 13 participants for all source-level analyses. Data and analysis scripts are available via the Donders Repository.

2.1 | MEG data analysis

The analyses were performed using FieldTrip version 20190922 (Oostenveld et al., 2011) in MATLAB R2017a. Figure 2 provides an overview of the MEG analysis pipeline. The original sampling rate was 1200 Hz and the data were down sampled to 600 Hz for computational efficiency, and then segmented into epochs from 1.4 s pre stimulus (i.e., the onset of the second-to-last blank screen) to 0.3 s post stimulus. In most cases, a function word (a determiner or a possessive pronoun) preceded the last blank screen. As in Piai et al. (2015), we analyzed the 800-ms interval (the last black screen) preceding the picture onset (Figure 1), during which response planning was reasoned to start following the constraining condition. This time window of interest is further motivated by prior results of time-resolved spectral power estimates in this paradigm (see Piai et al., 2014, 2015, 2020; Roos & Piai, 2020).

2.1.1 | MEG preprocessing

All MEG epochs were visually inspected for artefacts and in total 8.4% of the trials were excluded due to artefacts. Excessively noisy sensors were also removed. Artefacts- and error-free data comprised on average of 75.6 and 73.2 trials for the naming task and 79.4 and 79.6 for the judgment task, respectively, for the constraining and non-constraining contexts.

2.1.2 | Sensor-level analysis

The sensor-level analysis pipeline is shown on the left-hand side of Figure 2.

Spectral feature extraction on sensors

Rather than using predefined, canonical frequency bands that may not accurately capture the neural phenomenon of interest in each individual (Bazanova & Vernon, 2014; Haegens et al., 2014), an adaptive three-step approach was employed to define the frequencies of the alpha and beta peaks for each individual participant.

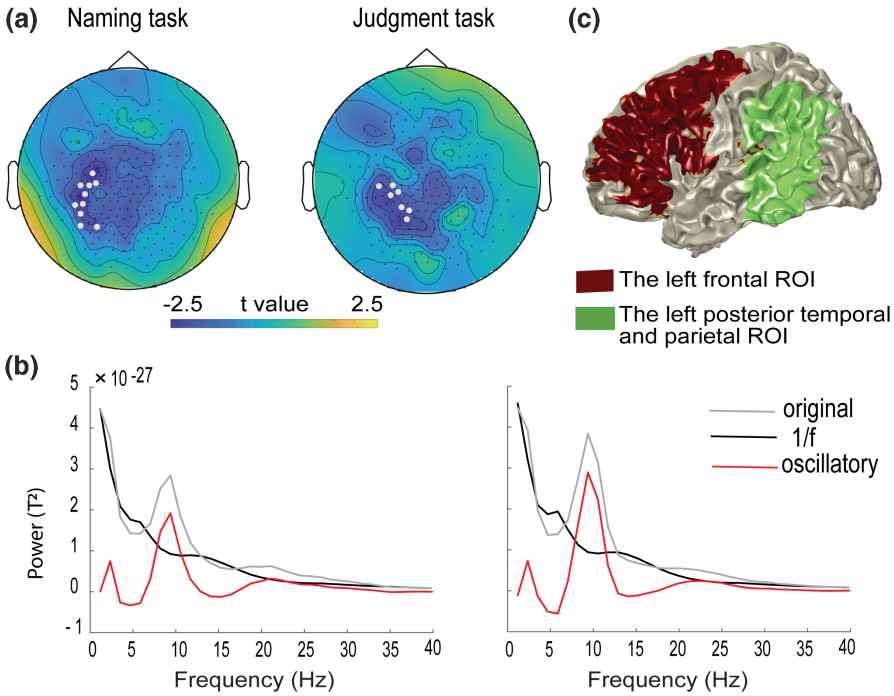

FIGURE 3 (a) The 10 representative sensors for the Naming task (left), and the seven representative sensors for the Judgment task (right) masked in grey shown in the scalp topographies. The topographies show averaged *t* values for the context effect (constraining vs. non-constraining) across the 15–25 Hz over the 800 ms time window of interest. (b) The power spectra averaged across the representative sensors for original power (grey line), 1/*f* component power (black line), and 1/*f* free oscillatory component power (red line) obtained from IRASA of Subject 17 in the Naming task (left) and Judgment task (right) as an example. (c) The two regions of interest (ROIs) in frontal and posterior temporo-parietal cortex selected to compare the power distribution similarity between alpha and beta

First, we selected the representative sensors that yielded a large context effect on the group level. For that, first, for the two tasks separately, power spectra were estimated in the 800-ms time window between 1 and 50 Hz for each sensor, condition, and participant, by applying the Fast Fourier Transform (FFT) on data tapered with a Hanning window (FieldTrip parameters "mtmfft" and "hanning"). Then, the significance of the differences in power between constraining and non-constraining context conditions was tested on the sensor level using non-parametric cluster-based permutation tests (Maris & Oostenveld, 2007). A single *t* value and its corresponding *p* value were calculated for each sensor-frequency bin pair between context conditions with a paired *t*-test. The sensors and frequency bins with paired *t*-test context effects exceeding a threshold ($p < .05$, two-tailed) were identified for the subsequent cluster test. The cluster-level statistic was defined as the sum of *t* values from the neighboring above-threshold sensors and frequency bins. Then, on the basis of 1000 random permutations of the two context conditions followed by the same clustering procedure, a distribution was created of the 1000 largest cluster-level statistics to test the null hypothesis that power in the two context conditions came from the same probability distribution. Given an alpha-level of 5% for the two-sided test, the null hypothesis was rejected if the empirical cluster-level statistic fell in the highest or lowest corresponding percentile of the permutation distribution (i.e., 2.5th percentile). The outcome of these (up to and including) steps are indicated as A1 in orange in Figure 2. To foreshadow the results, the cluster-based permutation tests revealed a significant difference between the two context conditions for each task, and the differences were most pronounced over the left temporo-parietal sensors. Subsequently, for the Naming and Judgment tasks separately, we selected the sensors that yielded a large context effect as the representative sensors in the following manner. We selected the sensors associated with the largest observed cluster whose averaged t-values between 15–25 Hz were more extreme than ±2 (see Figure 3a). These representative sensors were only used to help identify individual participants' alpha and beta frequency peaks, on which subsequent analyses were performed.

For each participant, and for each task separately, we used IRASA (Wen & Liu, 2016) for the signal collapsed across the two context conditions in the time window of interest, that is, the 800-ms interval between the last presented word and the onset of the picture, as indicated by "A2" in orange in Figure 2. IRASA allows distinguishing rhythmic activity from the concurrent arrhythmic 1/*f* modulation in the power spectrum of the neurophysiological signal. Subtracting the resulting 1/*f* spectrum from the

TABLE 1 Individual frequency peaks in Hz for each task and each frequency band defined on the 1/*f* free power spectra (osci) and on the original power spectra (orig) obtained from the procedures described for sensor-level analysis

	Naming task				Judgment task			
	Alpha		Beta		Alpha		Beta	
Participant	osci	orig	osci	orig	osci	orig	osci	orig
Sub1	10.5	10.5	14.0	15.2	10.5	10.5	14.0	15.2
Sub2	8.2	8.2	17.5	16.4	9.3	9.3	17.5	16.4
Sub5	10.5	9.3	17.5	14.0	10.5	10.5	21.0	16.4
Sub6	10.5	10.5	21.0	14.0	10.5	10.5	21.0	14.0
Sub7	10.5	10.5	21.0	14.0	10.5	10.5	19.9	14.0
Sub8	10.5	10.5	21.0	14.0	10.5	10.5	19.9	14.0
Sub11	9.3	9.3	18.7	17.5	9.3	9.3	11.7	12.8
Sub13	9.3	9.3	12.8	14.0	10.5	10.5	12.8	14.0
Sub14	11.7	11.7	23.4	16.4	11.7	11.7	23.4	15.2
Sub16	8.2	8.2	11.7	12.8	8.2	8.2	11.7	12.8
Sub17	9.3	9.3	21.0	14.0	9.3	9.3	22.2	14.0
Sub18	16.4	12.8	19.9	18.7	15.2	15.2	18.7	19.9
Sub19	11.7	11.7	23.4	15.2	11.7	11.7	23.4	15.2

Note: Note that, for four participants (i.e., Sub11, Sub13 and Sub16 for beta; Sub18 for alpha), the peak frequency fell outside the canonical frequency band for alpha (i.e., 8–12 Hz) and beta (i.e., 13–30 Hz).

original power spectrum offers a clearer estimation of the power spectrum of the rhythmic components. With this, we could address Consideration #1 (Donoghue et al., 2021) that the presence of an oscillation in the signal should be verified. Following the IRASA procedure, the peaks for alpha and beta were defined for each subject individually using the 1/*f* modulation-free power spectrum (see Stolk et al., 2019 for a similar approach). For that, we averaged the 1/*f* modulation-free power spectrum over the representative sensors defined above. We then inspected these power spectra to identify the spectrum shapes of alpha and beta (i.e., the presence of an inverse U-shaped power spectra for the alpha band, and no bump present for the beta band; see Figure 3b for an example). The mean and the full width at half maximum (FWHM) of the alpha spectral peak were defined for each participant by fitting a one-term Gaussian model. The peak frequency for beta was defined as the highest peak in the beta range, that is, not overlapping with alpha, at least 2 Hz higher than the individual participant's upper boundary of the alpha band and below 40 Hz. The outcome of these steps is indicated by "A3" in Figure 2. With this, Consideration #2 was addressed, namely, the fact that oscillations have variable peak frequencies calls for an individualized approach (Donoghue et al., 2021). On average, alpha and beta peaks were 10.5 ($SD = 2.0$) Hz and 18.8 ($SD = 3.7$) Hz for Naming and 10.6 ($SD = 1.6$) Hz and 18.3 ($SD = 4.2$) Hz for the Judgment task, respectively. Table 1 presents individual frequency peaks for alpha and beta for each task, both based on the 1/*f* modulation-free power spectra and on the original power spectra. It is clear that some peak frequencies are different between the two power spectra, especially in the beta range.

Context effect from oscillatory power spectra and trial-based spectral relations

To assure that the previously observed power decreases from the narrowband approach associated with the context effect reflect oscillatory activity (Consideration #3, Donoghue et al., 2021), we performed a cluster-based permutation test (as described above) on the 1/*f* free power spectra for constraining versus non-constraining conditions for each task separately (indicated as "A4" in Figure 2).

To assess whether the separation of alpha and beta bands with the IRASA approach was successful, a within-subject trial-by-trial correlation analysis was performed on the power at the peak frequencies for the alpha and beta bands based on the original power spectra and based on the 1/*f* free oscillatory power spectra defined in the former steps. If power at the peak alpha and beta frequencies correlates across trials, this could be attributed to either arrhythmic or rhythmic activity, especially because correlated patterns of change across frequency bands may be more parsimoniously explained as a change in broadband arrhythmic activity (Donoghue et al., 2021). The alpha-beta power decreases in the pre-picture interval were considered to reflect conceptual preparation and word-planning processes (Piai et al., 2015, 2020; Piai & Zheng, 2019), which can take place before picture onset only in the constraining condition, but not in the non-constraining condition. Thus, we

focused on the constraining condition for this analysis (see Roos & Piai, 2020). For each of the 13 participants individually, first, the correlation was computed in the following way: For each trial, the power at the peak frequencies was averaged across the representative sensors. Then, a Spearman correlation analysis was performed across trials between the participant's alpha and beta band power. This was done both for the original power spectra and for the 1/*f* free power spectra separately (i.e., power at alpha peak based on original power spectra correlated with power at beta peak based on original power spectra; power at alpha peak based on 1/*f* free power spectra correlated with power at beta peak based on 1/*f* free power spectra). This resulted in one array of 13 correlation coefficients for the original power spectra and one array for the 1/*f* free power spectra. These arrays were used for group-level analysis to assess the consistency of the correlation coefficients over participants. A one-sample *t*-test was employed to compare the mean correlation coefficient to zero (as indicated by "A5" in Figure 2).

2.1.3 | Source-level analysis

The source-level analysis pipeline is shown on the right-hand side of Figure 2.

Source reconstruction

We used beamforming to localize the sources of the alpha and beta band oscillations, respectively, over the 800-ms pre-picture interval. A frequency-domain beam-forming method (Dynamic Imaging of Coherent Sources, DICS) was used to identify sources of the alpha and beta oscillatory activity. The DICS technique uses adaptive spatial filters to localize power in the entire brain (Gross et al., 2001). Each filter has the property that it passes activity from the location of interest with unit gain, but maximally suppresses activities from other sources contributing to the data. To construct the spatial filters, we first constructed the forward model (lead-field matrix). For each subject, the anatomical MRI was segmented into brain, scalp, and skull using SPM8. From the segmented MRI, a realistic single-shell model of the inside of the skull was constructed which served as the individual volume conduction model (Nolte, 2003). Next, each individual's MRI was warped to a template MRI (Montreal Neurological Institute, MNI, Montreal, QC, Canada) and the source locations of grid points with a regular 10 mm spacing in the template model were mapped back from the MNI template to the individual's coordinates with an inverse warp. For each participant, this procedure resulted in individual grid points that were also matched to the MNI template coordinate system. The volume conduction model was then used to compute the lead-field matrix for each grid point. Next, we constructed the cross-spectral density matrix. For each participant, task, and frequency band (i.e., Naming alpha, Naming beta, Judgment alpha, Judgment beta), the sensor-level cross-spectral density matrices were computed by combing the data of the two context conditions (i.e., constraining and non-constraining) at the individuals' peak frequencies with a frequency smoothing of 2 Hz around the peak frequency. Using the cross-spectral density matrices and the lead-field matrices, a common spatial filter over constraining and non-constraining conditions was constructed for each task and for each frequency (i.e., Naming alpha, Naming beta, Judgment alpha, Judgment beta). The spatial filters were then applied to the Fourier transformed data from each context condition separately, allowing us to estimate the single trial source-level power for each grid point in each condition and each subject (indicated by "A6" in Figure 2). For each subject, the power estimates were then averaged over trials in each of the two context conditions. The relative power change was calculated as the difference between the power in the two conditions, divided by their average. To identify the cortical locations that were significantly modulated by the context effect, we performed non-parametric cluster-based permutation tests for constraining versus non-constraining conditions (Maris & Oostenveld, 2007), as explained above, resulting in a cluster of adjacent grid points exhibiting a similar context effect (indicated by "A7" in Figure 2).

For the analysis of spatial differences between alpha and beta with the earth mover's distance (see below), the data were divided into the following ROIs. Given previous findings on the context effect in word production (Piai et al., 2015, 2018; Roos & Piai, 2020) and existing models of language, which highlight the relevance of and distinction between frontal and temporal-parietal regions (Hickok & Poeppel, 2007; Indefrey & Levelt, 2004), we selected two regions of interest (ROIs) (see Figure 3c): left frontal cortex (152 grid points, labels in MNI template according to AAL atlas, Tzourio-Mazoyer et al., 2002): "Precentral_L", "Frontal_Sup_L", "Frontal_Mid_L", "Frontal_Inf_Oper_L", "Frontal_Inf_Tri_L", "Frontal_Inf_Orb_L", "Rolandic_Oper_L") and left posterior temporal and inferior parietal cortex (79 grid points, labels in MNI template according to AAL atlas): "Temporal_Sup_L", "Temporal_Pole_Sup_L", "Temporal_Mid_L", "Temporal_Pole_Mid_L", "Temporal_Inf_L", "Parietal_Inf_L", "SupraMarginal_L", "Angular_L", with the MNI coordinate $Y < 2$ cm for the border between posterior and anterior temporal lobe.

Source-level power distribution similarities between alpha and beta

To compare the spatial distribution of alpha and beta power, we used both a correlation-analysis approach and

the earth mover's distance (EMD), as indicated by "A8" in Figure 2. The EMD quantifies the minimal cost that is required to transform one distribution into another distribution (Rubner et al., 2000). The EMD was first introduced into the field of EEG/MEG as an inverse solution evaluation to measure spatial similarity between simulated and estimated source densities (Haufe et al., 2008).

In the EMD metaphor, the distributions can be seen as two different distributions of sand in two equally sized sandboxes. The EMD quantifies the least amount of work needed to turn one distribution into another one, where a unit of work corresponds to transporting a unit of sand by a unit of distance. The EMD can be computed by solving an instance of the transportation problem, using any algorithm for the minimum cost flow problem. For each task, and in each of the ROIs, we computed the EMD between the spatial distribution of alpha power and the spatial distribution of beta power, using the implementation of Rubner et al. (Yilmaz, 2021) with the Euclidean distance in 3D source space as the "ground distance" and the paired-sample *t*-statistic of the context effect on source power as the "amount of sand" at each grid point. The amount of positive and negative *t* values was highly comparable between alpha and beta for each task and ROI. The use of *t* values, rather than (raw) power, ensured that the values were standardized and weighted across participants, and comparable across tasks and frequency bands. The "amount of sand" in the EMD cannot be negative, but the *t* values are both positive and negative. We addressed the non-negative constraint for the EMD in the following way: Firstly, we "raised the bumps" for the two power distributions by adding a constant to the original *t* values. The minimum *t* value was −1.451 and −0.534 for the Naming task in Frontal and Temporal ROIs respectively, and −2.610 and −0.437 for the Judgment task in Frontal and Temporal ROIs, respectively. We lifted all the *t* values such that the minimum *t* value became 0.01. Secondly, to make the overall "mass" of the distributions equal, we divided the *t* values obtained from the last step by the sum of *t* values in the same distribution. Thus, for every distribution (i.e., both alpha and beta for each task and each ROI), the overall "mass" was made equal to 1.

In addition to the EMD computation, Pearson's correlation coefficients were computed to the same nonnegative "amount of sand" data to compare the similarity in spatial distribution between alpha and beta for each ROI and each task, with the units of observation corresponding to the grid points within the ROI. Note that this linearization analysis is only meant to provide converging evidence for the EMD findings. Both correlation coefficients and EMD are effect-size measures that serve as a quantitative reflection of the magnitude of the association. No inferential statistics is applied here, for statistical significance tests are traditionally used to provide evidence (attained *p* values) that a null hypothesis is false. However, there is no known distribution for EMD under the null hypothesis. Moreover, given the dependence in the data, a correlation coefficient does not match the null hypothesis, and therefore a probability calculated from these coefficients is likely inaccurate. Effect size and null hypothesis tests are conceptually independent and represent different ways of using data to make inferences (Kelley & Preacher, 2012). Under the hypothesis that the spatial distributions of alpha and beta bands are similar, one would expect a small EMD value and a large correlation coefficient. By contrast, if the spatial distributions are different, one would expect a large EMD value and a small correlation coefficient.

3 | RESULTS

3.1 | Context effects in the 1/*f* free oscillatory power

We assessed the presence of a context effect based on the 1/*f* free power spectra obtained after IRASA. Nonparametric cluster-based permutation tests rejected the hull hypothesis that power in the two conditions came from the same probability distribution (Naming: $p = .032$; Judgment: $p = .046$). Thus, we conclude that the context effect is present in the 1/*f* free oscillatory activity for both tasks.

We assessed the separation of alpha and beta oscillations using IRASA to remove the 1/*f* component in the power spectra. We found that, when the power at the peak frequency was defined on the original power spectra with the 1/*f* signal included, alpha and beta power were significantly positively correlated (one-sample *t*-test; $p < .001$). By contrast, when the power at the peak frequency was defined on the basis of the power spectra with the 1/*f* modulation removed, alpha and beta power showed no significant correlation ($p = .859$). Thus, the shared variance in the two frequency bands from the 1/*f* modulation was successfully accounted for by the application of IRASA.

3.2 | Source-Level analysis

Figure 4 shows the source localization of the context effect in the alpha and beta bands (based on individualized alpha and beta peaks estimated from the 1/*f* free oscillatory component) at the group-level, masked by the cluster associated with grid points below the cluster alpha-level threshold. Alpha power decreases for constrained relative to non-constrained context conditions were statistically significant for the Naming ($p = .002$) and Judgment tasks

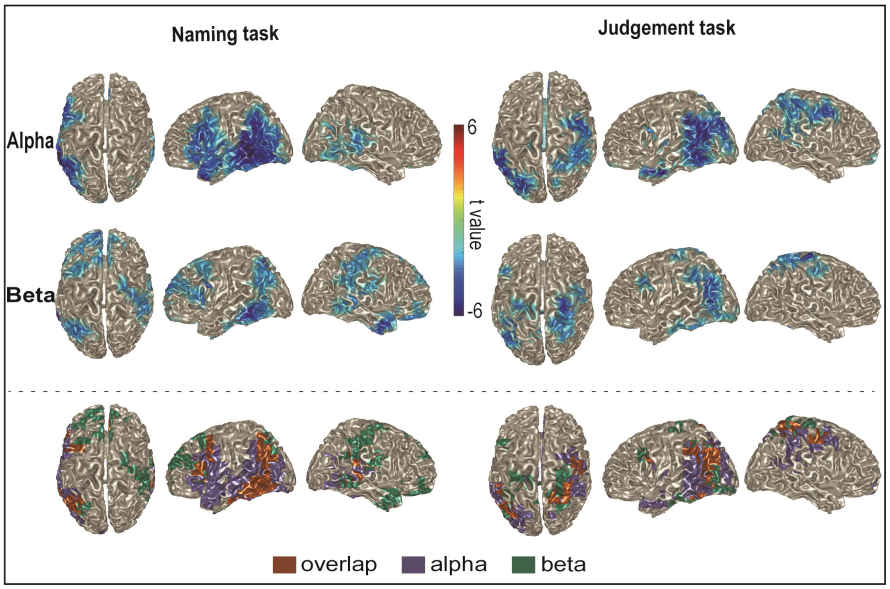

FIGURE 4 Group-level source localization of the power differences between peak frequencies ±2 Hz as a function of sentential constraint for the Naming task (left), Judgment task (right), for the alpha band (top rows) and beta band (middle rows). The color bar indicates the statistic *t* values. Overlap maps of group-level source localization are given in the bottom rows, showing areas of power changes common to both alpha and beta (brown), only for alpha (purple), and only for beta (green)

TABLE 2 Earth mover's distance (EMD) and Pearson correlation coefficients for each task in each of the two regions of interest, comparing alpha and beta power modulations

	Naming task		Judgment task	
	EMD	**Correlation**	**EMD**	**Correlation**
Left frontal	0.7745	0.1398	0.3496	0.4762
Left temporal-parietal	0.3662	0.4571	0.5423	0.2195

Note: Smaller EMD indicates stronger distribution similarity.

($p = .002$). Beta power decreases for constrained relative to non-constrained context conditions were statistically significant for the Naming (resulting in three clusters, $p = .044$; $p = .044$; $p = .050$) and Judgment tasks ($p = .002$). For each task, in Figure 4, the prominent clusters are depicted only for alpha, only for beta, and for their overlap.

Descriptively, for both the Naming and Judgment tasks, the alpha and beta power decreases overlapped in the left posterior temporal lobe extending into the left inferior parietal cortex. Compared with the Judgment task, both alpha and beta power decreases were also observed in a left frontal region in the Naming task. In the right hemisphere, the beta power decrease was observed more extensively than the alpha power decrease for the Naming task. Beta power decreases were observed around the right post-central gyrus and right temporal pole. For the Judgment task, both alpha and beta power decreases were observed around the right post-central and pre-central gyri (around the hand area in the sensorimotor cortex).

3.3 | Alpha and beta effects overlap in posterior left temporal-parietal regions

The qualitative assessment of the power distribution similarities between alpha and beta, shown above, was supported by converging results from the EMD analyses and correlation coefficients. The distances between alpha and beta power distributions for each task in each ROI, and the correlation coefficients between the nonnegative *t* values of alpha and beta on each grid point in the ROIs are presented in Table 2. A smaller EMD indicates a stronger resemblance of the distributions. A positive correlation indicates that the modulation of power decreases between the alpha and beta bands follows the same direction, with larger numbers indicating stronger relationships.

For the Judgment task, for both ROIs, the distributions of alpha and beta do not seem to vastly differ as evidenced by comparatively small EMDs and relatively comparable correlation coefficients of small to medium effect sizes (i.e., between 0.2 and 0.47). By contrast, for the Naming task, in left posterior temporo-parietal ROI, the alpha and beta have more similar distributions than the left frontal ROI, as indicated by a relatively smaller EMD value and a larger correlation coefficient of medium effect size. Interestingly, the magnitude of the EMDs and correlation coefficients was similar between the frontal ROI for the Judgment task, encompassing primary motor cortex, and the posterior ROI for the Naming task. Of note, the group-level results on the context-effect power modulations in the alpha and beta bands did not yield prominent clusters in the frontal ROI for the Judgment task, whereas for the Naming task, there were prominent group-level clusters for both alpha and beta in the posterior ROI (see Figure 4).

Both the EMD and correlation analyses were based on the *t*-values for each grid point in the ROIs, which reflect not only the magnitude of power modulation but also the consistency across participants. Thus, in the frontal ROI for the Judgment task, similar noise may drive the *t*-values for both alpha and beta, yielding a comparatively small EMD value and a large correlation coefficient in the absence of prominent clusters for the context effect in either alpha or beta bands. This issue limits a more direct comparison between these two sets of findings. Finally, the relatively smaller number of grid points in the posterior ROI than in the frontal ROI may represent a potential confound for the comparison of EMD and correlation coefficient values between the two ROIs. However, if that were the case, one would expect the frontal ROI to consistently yield more extreme values across the two tasks. This is not what we found, as the results go in opposite directions for the Judgment task and Naming tasks across the two ROIs. Thus, the number of grid points does not present a substantial confound for the interpretation of distribution similarity based on the EMD and coefficient values of the two ROIs. Still, making strong statements about the EMDs across ROIs is challenging.

4 | DISCUSSION

Alpha and beta power decreases have been consistently found in context-driven word production, thought to reflect conceptual and lexical retrieval processes (Gastaldon et al., 2020; Klaus et al., 2020; Piai et al., 2014, 2015, 2018, 2020; Roos & Piai, 2020). However, it remains unknown whether the robust power decreases over two "classical" (sensorimotor) frequency bands, namely alpha and beta, serve distinct roles in language production. In the motor domain, alpha and beta power decreases have been found to support motor preparation with spatiotemporal (Stolk et al., 2019) and functional (Brinkman et al., 2016; Wach et al., 2013) dissociations. These observations motivated the present study, in which we investigated the spatial distribution of the alpha and beta power decreases in language production. We reanalyzed MEG data of Piai et al. (2015) with the aim to assess the anatomical specificity of alpha- and beta-band rhythms in context-driven word production. We used the IRASA procedure to separate and measure aperiodic and periodic power and better isolate the alpha and beta bands (Wen & Liu, 2016). It is acknowledged that MEEG brain signals contain aperiodic activity, which shows as a decrease in power with increasing frequency in the power spectrum, characterized by a $1/f$ function. Aperiodic parameters (e.g., offset, exponent) differ across individuals (Donoghue et al., 2021). Standard narrow-band approaches can conflate aperiodic and periodic components (Donoghue et al., 2020). We found that the context effect is present in the periodic, $1/f$ free power spectra as defined by IRASA. Furthermore, we defined frequency peaks for alpha and beta based on the periodic component without the contribution of power from the aperiodic component, and source localized the context effects based on these alpha and beta bands. Lastly, EMD and correlation analyses were employed to quantify the spatial distribution similarity between alpha and beta sources. Power in the alpha and beta bands was correlated based on the original signal. By contrast, following the IRASA procedure with the $1/f$ modulation removed, alpha-band and beta-band power were no longer correlated (see also Stolk et al., 2019). This finding is interesting in itself and suggests that previous studies focusing on similarities between alpha- and beta-band power may have been confounded by their shared variance through the $1/f$ component.

We found that for both the Naming and Judgment tasks, the alpha and beta power decreases overlapped in the left posterior temporal lobe extending into the left inferior parietal cortex. The EMD and correlation analyses further suggested that the spatial distributions of alpha and beta power at the source level in left temporal and inferior parietal cortex were similar to the extent that we could assess it. By contrast, for the left frontal region, spanning the inferior, middle, and superior frontal gyri and the primary motor cortex, the power distributions differed between alpha and beta for the Naming task, but not for the Judgment task. The present results should be interpreted in light of our previous findings of well-established, robust, and replicable power decreases in the alpha and beta bands for the naming task (e.g., Klaus et al., 2020; Piai et al., 2015, 2018; Roos & Piai, 2020), providing more confidence that the EMD and correlation findings are not driven (solely) by noise. For example, the present results are consistent with previous findings that alpha-beta oscillations in left frontal cortex for context-driven word production are less critical (Piai et al., 2018) and less consistent (Roos & Piai, 2020) than in left temporal and inferior parietal cortex. Piai et al. (2018) provided lesion evidence for a critical role of left posterior but not left frontal areas in alpha-beta power decreases in context-driven word production. Using the same naming task as in the present study, the absence of a context-induced behavioral facilitation effect co-occurred with an absent alpha-beta context effect in stroke patients with extensive left-hemisphere posterior lesions. By contrast, both effects were present in the stroke patients with left-hemisphere frontal lesions. With healthy young adults, Roos and Piai (2020) used the same naming task in two test-retest sessions that only differed in the stimulus materials. The same participants performed the naming task at two time points around 14 to 28 days apart. The alpha-beta

power decreases in left temporal and inferior parietal cortices were found consistently across both sessions, whereas the involvement of left middle frontal gyrus was only found in session 2, but not in session 1.

For both Naming and Judgment tasks, the pre-picture intervals were reasoned to involve conceptual activation following constraining contexts. The context effect on left posterior temporal and inferior parietal cortex observed in both tasks is consistent with the proposed roles of these regions from multiple studies using different neuroimaging modalities, such as angular gyrus and portions of supramarginal gyrus in conceptual processing (for a review, see Binder et al., 2009) and left mid-posterior middle temporal gyrus and left posterior inferior temporal gyrus in lexical-semantic retrieval during picture naming (Baldo et al., 2013; Liljeström et al., 2008; for a general review, see Price, 2012). By contrasting the two tasks in this posterior ROI, it is noticeable that the Judgment task had a bigger EMD and a smaller correlation coefficient than the Naming task. Accordingly, it could be argued that this finding supports the conclusion that for conceptual-lexical retrieval, alpha and beta oscillations do dissociate. In our paradigm, spreading activation in the lexical-semantic network in constraining sentence contexts supports the retrieval of the pictured concept, which is present for both tasks. By contrast, compared with the Naming task, lexical information may have been less prominent in the pre-picture interval for the Judgment task, as the latter task can in principle be performed without lexical access. Our EMD and correlation analyses were based on the *t* values of the context effect, which reflect both the magnitude of the effect and consistency across trials and participants. The posterior ROI included both inferior parietal regions associated with conceptual processing and posterior temporal regions associated with lexical retrieval. Thus, the posterior ROI may have a combination of areas whose functions are not equally represented in both tasks, yielding a smaller EMD and a bigger correlation coefficient for the Naming than for the Judgment task.

Previous electrophysiological studies have suggested a role for alpha–beta power decreases in lexical retrieval (e.g., Brennan et al., 2014; Mellem et al., 2012; Piai et al., 2015, 2020). The present study further shows that the alpha- and beta-band oscillations have similar power distributions in the brain regions associated with conceptual preparation, and also possibly with lexical retrieval. Thus, the replicable alpha-beta power decreases in context-driven word production may index an oscillatory signature underlying one sole process, conceptual-lexical activation or retrieval. This hypothesis would also be in line with a theoretical view in the field of episodic memory that provides a mechanistic explanation for the alpha-beta power decreases in the encoding and retrieval of episodic information. According to this view, information is encoded by neuronal desynchronization in the neocortex (Hanslmayr et al., 2012). This information-based mechanistic account of alpha/beta power decreases may also hold for conceptually driven lexical-semantic retrieval (see also Fellner et al., 2013; Piai et al., 2020; Piai & Zheng, 2019).

Compared with the Judgment task, the Naming task elicited more left frontal power decreases. The left inferior frontal gyrus (LIFG) has been recognized as an important region not only for language but also for other cognitive functions. Our observation of LIFG and, adjacently, left premotor cortex involvement in the Naming but not in the Judgment task would be compatible with the phonological and phonetic (Indefrey & Levelt, 2004; Smith & Jonides, 1999) accounts of LIFG, because phonological and phonetic information are needed in the Naming task, but not in the Judgment task. However, the extent to which participants already prepare a phonological or phonetic code during the pre-picture interval is unclear. LIFG involvement only in the Naming but not in the Judgment task would also be compatible with a recent claim that the involvement of LIFG in language comprehension and production is asymmetric (Matchin & Hickok, 2020). According to the reviewed neurological literature that lesion-deficit mapping studies reveal a more robust association between brain lesions in LIFG with agrammatic production than comprehension, these authors proposed that the role of the LIFG in language is to transform the information from posterior middle temporal gyrus into a linear sequence of morphemes, and is thus primarily tied to production. However, we acknowledge that the separation of comprehension and production as modules is a complex issue.

Alpha and beta frontal effects have been reported in language production studies with various paradigms (e.g., auditory description naming and picture naming with MEG, Youssofzadeh et al., 2020) in addition to context-driven word production (from EEG, Gastaldon et al., 2020). As indicated by the EMD and correlation coefficient analyses, the alpha- and beta-band oscillations have different power distributions for the Naming task in our frontal ROI, which encompasses LIFG and motor cortex. As can be seen in Figure 4, more pronounced alpha than beta oscillations were present around LIFG, while more pronounced beta than alpha oscillations were present around superior and middle frontal gyri. Naming involves a cascade from phonological retrieval to phonetic encoding operating on an abstract phonological representation. Our frontal ROI covering the left phonological-phonetic network may be argued to show a dissociation between alpha and beta bands from inferior (alpha) to superior (beta) frontal regions. Previous studies in the motor domain have indicated a more direct relationship for beta

than for alpha with motor processes. For instance, somatotopic organization (Salmelin et al., 1995) and coherence with the electromyogram (Brown, 2000; Mima & Hallett, 1999) were usually found for the beta, rather than for the alpha, band. For language production, studies have also found somatotopic arrangement in the motor cortex of the speech articulators (i.e., lips, jaw and tongue; for a review, see Conant et al., 2014), and beta-band power decreases around the bilateral face area in the motor cortex for a verbal task (Salmelin & Sams, 2002). Future studies could address the extent to which alpha, but not beta, in the LIFG could support more abstract (phonological) processes, whereas beta in motor areas could support motor programming for articulation.

For the right hemisphere, both alpha and beta power decreases for the Judgment task were observed around the precentral and postcentral gyri. Power decreases in the alpha and beta frequency bands over sensorimotor areas have been well characterized during preparation and execution of movement (for a review, see Cheyne, 2013). Because the participants were instructed to press a button with their left hands to respond after picture onset in the Judgment task, the observed alpha and beta decreases around the right motor area likely reflect the left-hand preparatory motor activity. By contrast, for the Naming task, both alpha and beta power decreases were observed around the right posterior superior temporal gyrus (pSTG) and supramarginal gurus (SMG), whose left hemisphere homologous regions are well documented as language-related areas. The pSTG has also been found to be bilaterally associated with lexical semantic processing (Senaha et al., 2005; Wright et al., 2012), and the SMG bilaterally with phonological processing (Hartwigsen et al., 2010) and verbal working memory (Deschamps et al., 2014) in healthy right-handed adults. Because the involvement in the right hemisphere was weaker than in the left in our study, it could explain why we got weaker overlap between alpha and beta in the right hemisphere. No EMD analysis was performed on the right-hemisphere counterpart of the posterior ROI for a quantitative measure of the distribution similarity. An EMD analysis serves to provide a quantitative measure of the distribution similarity in regions where both alpha and beta were present, and in the right hemisphere this overlap is very limited (see Figure 4).

When comparing the alpha and beta bands, in the Naming task, beta seems to be more present in the right hemisphere than alpha. In addition to the strip around the right premotor area mentioned above, power decreases were observed in the right anterior temporal lobe (ATL) for beta, but not for alpha. By contrast, alpha power decreases were observed in the left ATL. Our finding that beta oscillations are found in the right ATL during naming is consistent with an intracranial EEG study that found some ATL recording sites showing beta power decrease during name retrieval, and a relatively higher proportion of beta decreases from the right ATL than from left ATL (Abel et al., 2016). Bilateral ATLs have been suggested to underpin conceptual knowledge (Lambon Ralph & Patterson, 2008; Lambon Ralph et al., 2009), although it is unclear whether the two ATLs function in the same way. Patient studies have shown differences in performance between left and right ATL lesions: both left and right temporal lobe patients showed degraded comprehension, but left ATL patients showed weaker performance on tasks requiring naming (Lambon Ralph et al., 2001; Rice et al., 2018). Thus, to explain the asymmetry deficits of bilateral ATL lesions, an ATL-connection view has been put forward according to which the left ATL has stronger connectivity with the left-lateralized speech-production system. Previous fMRI studies have shown that resting-state functional connectivity (Hurley et al., 2014) and white matter connectivity (Leng et al., 2016) between ATL and IFG are higher in the left than in the right hemisphere. In our Naming task, alpha power decreases were found in the left ATL and in left IFG. Our findings using MEG provide tentative evidence that left ATL and left IFG are linked in word production through a common oscillation frequency band.

4.1 | Limitations

We acknowledge that there are limitations in our interpretation of the overlap or dissociation between alpha and beta oscillations in language production. The first limitation comes from the spatial resolution of MEG and the source localization procedure. MEG may not distinguish well two sources that have similar current flow orientations within 20 mm distance (Liljeström et al., 2005). Thus, our findings would ideally be confirmed using a method with higher spatial resolution, like intracranial EEG. Second, as shown in Figure 3, the power spectra of alpha and beta in our data have different shapes: a reverse-"U"-shaped power spectrum for the alpha band, but no evident peak in the thus-defined beta band. Given the lack of a dominant frequency in the beta range, one could question whether this component is truly oscillatory. Brain oscillations typically appear as bumps on top of the $1/f$ slope in a power spectrum, but there is a chance that the bump is difficult to detect when the oscillation amplitude is smaller than the $1/f$ slope in the corresponding frequency range (He, 2014). An additional limitation is that the source localization was not based on the $1/f$ free oscillatory signal, but on raw power instead. Care was taken, however, that alpha and beta bands were separated as much as possible for each individual participant.

Finally, in the present study, we could not address the (lack of) overlap in function between alpha and beta bands, but focused instead on the overlap in spatial distribution between these two bands. One could argue that the very fact that these are two different frequency bands already implies that they serve two different functions. However, this claim hinges strongly on how one defines a cognitive function, which is a question that deserves a research program in its own right and cannot be answered within one study.

5 | CONCLUSIONS

Our results show that for the robustly observed alpha- and beta-band power decreases in context-driven word production, the power for the peak frequencies of alpha and beta bands were not correlated when accounted for the 1/*f* modulation. For both the Naming and Judgment tasks, the power decreases in individualized alpha and beta bands overlapped in the left posterior temporal lobe extending into the left inferior parietal cortex. These areas have been associated with conceptual and lexical processing, and participants likely engaged in these processes given the information provided by the constraining sentences. The similar spatial distributions between alpha and beta bands for this posterior region, even when controlling for the arrhythmic 1/*f* component as much as possible in the estimation of alpha and beta peak frequencies, suggest that for conceptual and lexical processing, alpha and beta oscillations do not spatially dissociate.

ACKNOWLEDGMENT

We thank Arjen Stolk, Eric Maris, Natascha Roos, and Rui Liu for helpful discussions.

AUTHOR CONTRIBUTIONS

Yang Cao: Data curation; Formal analysis; Investigation; Methodology; Writing – original draft. **Robert Oostenveld:** Methodology; Validation; Writing – review & editing. **Phillip M. Alday:** Validation; Writing – review & editing. **Vitoria Piai:** Conceptualization; Data curation; Funding acquisition; Investigation; Methodology; Project administration; Supervision; Writing – review & editing.

ORCID

Yang Cao https://orcid.org/0000-0003-1057-7666
Robert Oostenveld https://orcid.org/0000-0002-1974-1293
Phillip M. Alday https://orcid.org/0000-0002-9984-5745
Vitória Piai https://orcid.org/0000-0002-4860-5952

REFERENCES

Abel, T. J., Rhone, A. E., Nourski, K. V., Ando, T. K., Oya, H., Kovach, C. K., Kawasaki, H., Howard, M. A., & Tranel, D. (2016). Beta modulation reflects name retrieval in the human anterior temporal lobe: An intracranial recording study. *Journal of Neurophysiology*, *115*(6), 3052–3061. https://doi.org/10.1152/jn.00012.2016

Baldo, J. V., Arévalo, A., Patterson, J. P., & Dronkers, N. F. (2013). Grey and white matter correlates of picture naming: Evidence from a voxel based lesion analysis of the Boston Naming Test. *Cortex*, *49*(3), 658–667. https://doi.org/10.1016/j.cortex.2012.03.001

Bazanova, O. M., & Vernon, D. (2014). Interpreting EEG alpha activity. *Neuroscience & Biobehavioral Reviews*, *44*, 94–110. https://doi.org/10.1016/j.neubiorev.2013.05.007

Binder, J. R., Desai, R. H., Graves, W. W., & Conant, L. L. (2009). Where is the semantic system? A critical review and meta-analysis of 120 functional neuroimaging studies. *Cerebral Cortex*, *19*(12), 2767–2796. https://doi.org/10.1093/cercor/bhp055

Brennan, J., Lignos, C., Embick, D., & Roberts, T. P. L. (2014). Spectro-temporal correlates of lexical access during auditory lexical decision. *Brain and Language*, *133*, 39–46. https://doi.org/10.1016/j.bandl.2014.03.006

Brinkman, L., Stolk, A., Dijkerman, H. C., de Lange, F. P., & Toni, I. (2014). Distinct roles for alpha- and beta-band oscillations during mental simulation of goal-directed actions. *Journal of Neuroscience*, *34*(44), 14783–14792. https://doi.org/10.1523/JNEUROSCI.2039-14.2014

Brinkman, L., Stolk, A., Marshall, T. R., Esterer, S., Sharp, P., Dijkerman, H. C., de Lange, F. P., & Toni, I. (2016). Independent causal contributions of alpha- and beta-band oscillations during movement selection. *Journal of Neuroscience*, *36*(33), 8726–8733. https://doi.org/10.1523/JNEUROSCI.0868-16.2016

Brown, P. (2000). Cortical drives to human muscle: The Piper and related rhythms. *Progress in Neurobiology*, *60*(1), 97–108. https://doi.org/10.1016/S0301-0082(99)00029-5

Buzsáki, G., & Draguhn, A. (2004). Neuronal oscillations in cortical networks. *Science*, *304*(5679), 1926–1929. https://doi.org/10.1126/science.1099745

Cheyne, D. O. (2013). MEG studies of sensorimotor rhythms: A review. *Experimental Neurology*, *245*, 27–39. https://doi.org/10.1016/j.expneurol.2012.08.030

Conant, D., Bouchard, K. E., & Chang, E. F. (2014). Speech map in the human ventral sensory-motor cortex. *Current Opinion in Neurobiology*, *24*, 63–67. https://doi.org/10.1016/j.conb.2013.08.015

Crone, N. E., & Hao, L. (2002). Functional dynamics of spoken and signed word production: A case study using electrocorticographic spectral analysis. *Aphasiology*, *16*(9), 903–927. https://doi.org/10.1080/02687030244000383

Crone, N. E., Miglioretti, D. L., Gordon, B., Sieracki, J. M., Wilson, M. T., Uematsu, S., & Lesser, R. P. (1998). Functional mapping of human sensorimotor cortex with electrocorticographic spectral analysis. I. Alpha and beta event-related desynchronization. *Brain*, *121*(12), 2271–2299. https://doi.org/10.1093/brain/121.12.2271

De Lange, F. P., Jensen, O., Bauer, M., & Toni, I. (2008). Interactions between posterior gamma and frontal alpha/beta oscillations

during imagined actions. *Frontiers in Human Neuroscience*, *2*, 7. https://doi.org/10.3389/neuro.09.007.2008

Dell, G. S., Burger, L. K., & Svec, W. R. (1997). Language production and serial order: A functional analysis and a model. *Psychological Review*, *104*(1), 123–147. https://doi.org/10.1037/0033-295X.104.1.123

Deschamps, I., Baum, S. R., & Gracco, V. L. (2014). On the role of the supramarginal gyrus in phonological processing and verbal working memory: Evidence from rTMS studies. *Neuropsychologia*, *53*, 39–46. https://doi.org/10.1016/j.neuropsychologia.2013.10.015

Donoghue, T., Haller, M., Peterson, E. J., Varma, P., Sebastian, P., Gao, R., Noto, T., Lara, A. H., Wallis, J. D., Knight, R. T., Shestyuk, A., & Voytek, B. (2020). Parameterizing neural power spectra into periodic and aperiodic components. *Nature Neuroscience*, *23*(12), 1655–1665. https://doi.org/10.1038/s41593-020-00744-x

Donoghue, T., Schaworonkow, N., & Voytek, B. (2021). Methodological considerations for studying neural oscillations. *European Journal of Neuroscience*, 1–26. https://doi.org/10.1111/ejn.15361

Fellner, M.-C., Bäuml, K.-H.- T., & Hanslmayr, S. (2013). Brain oscillatory subsequent memory effects differ in power and long-range synchronization between semantic and survival processing. *NeuroImage*, *79*, 361–370. https://doi.org/10.1016/j.neuroimage.2013.04.121

Friederici, A. D., & Singer, W. (2015). Grounding language processing on basic neurophysiological principles. *Trends in Cognitive Sciences*, *19*(6), 329–338. https://doi.org/10.1016/j.tics.2015.03.012

Gastaldon, S., Arcara, G., Navarrete, E., & Peressotti, F. (2020). Commonalities in alpha and beta neural desynchronizations during prediction in language comprehension and production. *Cortex*, *133*, 328–345. https://doi.org/10.1016/j.cortex.2020.09.026

Gross, J., Kujala, J., Hämäläinen, M., Timmermann, L., Schnitzler, A., & Salmelin, R. (2001). Dynamic imaging of coherent sources: Studying neural interactions in the human brain. *Proceedings of the National Academy of Sciences*, *98*(2), 694–699. https://doi.org/10.1073/pnas.98.2.694

Haegens, S., Cousijn, H., Wallis, G., Harrison, P. J., & Nobre, A. C. (2014). Inter- and intra-individual variability in alpha peak frequency. *NeuroImage*, *92*, 46–55. https://doi.org/10.1016/j.neuroimage.2014.01.049

Hanslmayr, S., Staudigl, T., & Fellner, M.-C. (2012). Oscillatory power decreases and long-term memory: The information via desynchronization hypothesis. *Frontiers in Human Neuroscience*, *6*, 74. https://doi.org/10.3389/fnhum.2012.00074

Hartwigsen, G., Baumgaertner, A., Price, C. J., Koehnke, M., Ulmer, S., & Siebner, H. R. (2010). Phonological decisions require both the left and right supramarginal gyri. *Proceedings of the National Academy of Sciences*, *107*(38), 16494–16499. https://doi.org/10.1073/pnas.1008121107

Haufe, S., Nikulin, V. V., Ziehe, A., Müller, K.-R., & Nolte, G. (2008). Combining sparsity and rotational invariance in EEG/MEG source reconstruction. *NeuroImage*, *42*(2), 726–738. https://doi.org/10.1016/j.neuroimage.2008.04.246

He, B. J. (2014). Scale-free brain activity: Past, present, and future. *Trends in Cognitive Sciences*, *18*(9), 480–487. https://doi.org/10.1016/j.tics.2014.04.003

Hickok, G., & Poeppel, D. (2007). The cortical organization of speech processing. *Nature Reviews Neuroscience*, *8*(5), 393–402. https://doi.org/10.1038/nrn2113

Hurley, R. S., Bonakdarpour, B., Wang, X., & Mesulam, M.-M. (2014). Asymmetric connectivity between the anterior temporal lobe and the language network. *Journal of Cognitive Neuroscience*, *27*(3), 464–473. https://doi.org/10.1162/jocn_a_00722

Indefrey, P., & Levelt, W. J. M. (2004). The spatial and temporal signatures of word production components. *Cognition*, *92*(1), 101–144. https://doi.org/10.1016/j.cognition.2002.06.001

Jurkiewicz, M. T., Gaetz, W. C., Bostan, A. C., & Cheyne, D. (2006). Post-movement beta rebound is generated in motor cortex: Evidence from neuromagnetic recordings. *NeuroImage*, *32*(3), 1281–1289. https://doi.org/10.1016/j.neuroimage.2006.06.005

Karakaş, S., & Barry, R. J. (2017). A brief historical perspective on the advent of brain oscillations in the biological and psychological disciplines. *Neuroscience & Biobehavioral Reviews*, *75*, 335–347. https://doi.org/10.1016/j.neubiorev.2016.12.009

Kelley, K., & Preacher, K. J. (2012). On effect size. *Psychological Methods*, *17*, 137–152. https://doi.org/10.1037/a0028086

Klaus, J., Schutter, D. J. L. G., & Piai, V. (2020). Transient perturbation of the left temporal cortex evokes plasticity-related reconfiguration of the lexical network. *Human Brain Mapping*, *41*(4), 1061–1071. https://doi.org/10.1002/hbm.24860

Lambon Ralph, M. A., McClelland, J. L., Patterson, K., Galton, C. J., & Hodges, J. R. (2001). No right to speak? The relationship between object naming and semantic impairment: Neuropsychological evidence and a computational model. *Journal of Cognitive Neuroscience*, *13*(3), 341–356. https://doi.org/10.1162/08989290151137395

Lambon Ralph, M. A., & Patterson, K. (2008). Generalization and differentiation in semantic memory: Insights from semantic dementia. *Annals of the New York Academy of Sciences*, *1124*, 61–76. https://doi.org/10.1196/annals.1440.006

Lambon Ralph, M. A., Pobric, G., & Jefferies, E. (2009). Conceptual knowledge is underpinned by the temporal pole bilaterally: Convergent evidence from rTMS. *Cerebral Cortex*, *19*(4), 832–838. https://doi.org/10.1093/cercor/bhn131

Lehtelä, L., Salmelin, R., & Hari, R. (1997). Evidence for reactive magnetic 10-Hz rhythm in the human auditory cortex. *Neuroscience Letters*, *222*(2), 111–114. https://doi.org/10.1016/S0304-3940(97)13361-4

Leng, B., Han, S., Bao, Y., Zhang, H., Wang, Y., Wu, Y., & Wang, Y. (2016). The uncinate fasciculus as observed using diffusion spectrum imaging in the human brain. *Neuroradiology*, *58*(6), 595–606. https://doi.org/10.1007/s00234-016-1650-9

Levelt, W. J. M., Roelofs, A., & Meyer, A. S. (1999). A theory of lexical access in speech production. *Behavioral and Brain Sciences*, *22*, 1–38. https://doi.org/10.1017/S0140525X99001776

Liljeström, M., Kujala, J., Jensen, O., & Salmelin, R. (2005). Neuromagnetic localization of rhythmic activity in the human brain: A comparison of three methods. *NeuroImage*, *25*(3), 734–745. https://doi.org/10.1016/j.neuroimage.2004.11.034

Liljeström, M., Tarkiainen, A., Parviainen, T., Kujala, J., Numminen, J., Hiltunen, J., Laine, M., & Salmelin, R. (2008). Perceiving and naming actions and objects. *NeuroImage*, *41*(3), 1132–1141. https://doi.org/10.1016/j.neuroimage.2008.03.016

Maris, E., & Oostenveld, R. (2007). Nonparametric statistical testing of EEG- and MEG-data. *Journal of Neuroscience Methods*, *164*(1), 177–190. https://doi.org/10.1016/j.jneumeth.2007.03.024

Matchin, W., & Hickok, G. (2020). The cortical organization of syntax. *Cerebral Cortex*, *30*(3), 1481–1498. https://doi.org/10.1093/cercor/bhz180

Mellem, M., Bastiaansen, M., Pilgrim, L., Medvedev, A., & Friedman, R. (2012). Word class and context affect alpha-band oscillatory dynamics in an older population. *Frontiers in Psychology*, *3*, 1–8. https://doi.org/10.3389/fpsyg.2012.00097

Mima, T., & Hallett, M. (1999). Corticomuscular coherence: A review. *Journal of Clinical Neurophysiology*, *16*(6), 501–511. https://doi.org/10.1097/00004691-199911000-00002

Niedermeyer, E. (1993). The "Third Rhythm": Alpha-like activity over the midtemporal region. *American Journal of EEG Technology*, *33*(3), 159–173. https://doi.org/10.1080/00029238.1993.11080446

Nolte, G. (2003). The magnetic lead field theorem in the quasi-static approximation and its use for magnetoencephalography forward calculation in realistic volume conductors. *Physics in Medicine & Biology*, *48*(22), 3637. https://doi.org/10.1088/0031-9155/48/22/002

Nyhus, E., & Curran, T. (2010). Functional role of gamma and theta oscillations in episodic memory. *Neuroscience & Biobehavioral Reviews*, *34*(7), 1023–1035. https://doi.org/10.1016/j.neubiorev.2009.12.014

Oostenveld, R., Fries, P., Maris, E., & Schoffelen, J.-M. (2011). FieldTrip: Open source software for advanced analysis of MEG, EEG, and invasive electrophysiological data. *Computational Intelligence and Neuroscience*, *2011*, e156869. https://doi.org/10.1155/2011/156869

Pfurtscheller, G., Neuper, C., Andrew, C., & Edlinger, G. (1997). Foot and hand area mu rhythms. *International Journal of Psychophysiology*, *26*(1), 121–135. https://doi.org/10.1016/S0167-8760(97)00760-5

Piai, V., Klaus, J., & Rossetto, E. (2020). The lexical nature of alpha-beta oscillations in context-driven word production. *Journal of Neurolinguistics*, *55*, e100905. https://doi.org/10.1016/j.jneuroling.2020.100905

Piai, V., Meyer, L., Dronkers, N. F., & Knight, R. T. (2017). Neuroplasticity of language in left-hemisphere stroke: Evidence linking subsecond electrophysiology and structural connections. *Human Brain Mapping*, *38*(6), 3151–3162. https://doi.org/10.1002/hbm.23581

Piai, V., Roelofs, A., & Maris, E. (2014). Oscillatory brain responses in spoken word production reflect lexical frequency and sentential constraint. *Neuropsychologia*, *53*, 146–156. https://doi.org/10.1016/j.neuropsychologia.2013.11.014

Piai, V., Roelofs, A., Rommers, J., & Maris, E. (2015). Beta oscillations reflect memory and motor aspects of spoken word production. *Human Brain Mapping*, *36*(7), 2767–2780. https://doi.org/10.1002/hbm.22806

Piai, V., Rommers, J., & Knight, R. T. (2018). Lesion evidence for a critical role of left posterior but not frontal areas in alpha–beta power decreases during context-driven word production. *European Journal of Neuroscience*, *48*(7), 2622–2629. https://doi.org/10.1111/ejn.13695

Piai, V., & Zheng, X. (2019). Speaking waves: Neuronal oscillations in language production. In K. D. Federmeier (Ed.), *Psychology of learning and motivation* (Vol. *71*, pp. 265–302). Academic Press.

Price, C. J. (2012). A review and synthesis of the first 20 years of PET and fMRI studies of heard speech, spoken language and reading. *NeuroImage*, *62*(2), 816–847. https://doi.org/10.1016/j.neuroimage.2012.04.062

Rice, G. E., Caswell, H., Moore, P., Hoffman, P., & Lambon Ralph, M. A. (2018). The roles of left versus right anterior temporal lobes in semantic memory: A neuropsychological comparison of postsurgical temporal lobe epilepsy patients. *Cerebral Cortex*, *28*(4), 1487–1501. https://doi.org/10.1093/cercor/bhx362

Roos, N. M., & Piai, V. (2020). Across-session consistency of context-driven language processing: A magnetoencephalography study. *European Journal of Neuroscience*, *52*(5), 3457–3469. https://doi.org/10.1111/ejn.14785

Rubner, Y., Tomasi, C., & Guibas, L. J. (2000). The earth mover's distance as a metric for image retrieval. *International Journal of Computer Vision*, *40*(2), 99–121. https://doi.org/10.1023/A:1026543900054

Salmelin, R., Hámáaláinen, M., Kajola, M., & Hari, R. (1995). Functional segregation of movement-related rhythmic activity in the human brain. *NeuroImage*, *2*(4), 237–243. https://doi.org/10.1006/nimg.1995.1031

Salmelin, R., & Sams, M. (2002). Motor cortex involvement during verbal versus non-verbal lip and tongue movements. *Human Brain Mapping*, *16*(2), 81–91. https://doi.org/10.1002/hbm.10031

Salmelin, R., Schnitzler, A., Schmitz, F., & Freund, H. J. (2000). Single word reading in developmental stutterers and fluent speakers. *Brain*, *123*(6), 1184–1202. https://doi.org/10.1093/brain/123.6.1184

Sederberg, P. B., Kahana, M. J., Howard, M. W., Donner, E. J., & Madsen, J. R. (2003). Theta and gamma oscillations during encoding predict subsequent recall. *Journal of Neuroscience*, *23*(34), 10809–10814. https://doi.org/10.1523/JNEUROSCI.23-34-10809.2003

Senaha, M. L. H., Martin, M. G. M., Amaro, E., Campi, C., & Caramelli, P. (2005). Patterns of cerebral activation during lexical and phonological reading in Portuguese. *Brazilian Journal of Medical and Biological Research*, *38*(12), 1847–1856. https://doi.org/10.1590/s0100-879x2005001200013

Smith, E. E., & Jonides, J. (1999). Storage and executive processes in the frontal lobes. *Science*, *283*(5408), 1657–1661. https://doi.org/10.1126/science.283.5408.1657

Stolk, A., Brinkman, L., Vansteensel, M. J., Aarnoutse, E., Leijten, F. S. S., Dijkerman, C. H., Knight, R. T., de Lange, F. P., & Toni, I. (2019). Electrocorticographic dissociation of alpha and beta rhythmic activity in the human sensorimotor system. *eLife*, *8*, e48065. https://doi.org/10.7554/eLife.48065

Szurhaj, W., Derambure, P., Labyt, E., Cassim, F., Bourriez, J.-L., Isnard, J., Guieu, J.-D., & Mauguière, F. (2003). Basic mechanisms of central rhythms reactivity to preparation and execution of a voluntary movement: A stereoelectroencephalographic study. *Clinical Neurophysiology*, *114*(1), 107–119. https://doi.org/10.1016/S1388-2457(02)00333-4

Tiihonen, J., Kajola, M., & Hari, R. (1989). Magnetic mu rhythm in man. *Neuroscience*, *32*(3), 793–800. https://doi.org/10.1016/0306-4522(89)90299-6

Tzourio-Mazoyer, N., Landeau, B., Papathanassiou, D., Crivello, F., Etard, O., Delcroix, N., Mazoyer, B., & Joliot, M. (2002). Automated anatomical labeling of activations in SPM using a macroscopic anatomical parcellation of the MNI MRI single-subject brain. *NeuroImage*, *15*(1), 273–289. https://doi.org/10.1006/nimg.2001.0978

Wach, C., Krause, V., Moliadze, V., Paulus, W., Schnitzler, A., & Pollok, B. (2013). Effects of 10Hz and 20Hz transcranial alternating current stimulation (TACS) on motor functions and motor cortical excitability. *Behavioural Brain Research*, *241*, 1–6. https://doi.org/10.1016/j.bbr.2012.11.038

Wang, L., Hagoort, P., & Jensen, O. (2017). Language prediction is reflected by coupling between frontal gamma and posterior alpha oscillations. *Journal of Cognitive Neuroscience*, *30*(3), 432–447. https://doi.org/10.1162/jocn_a_01190

Wang, L., Jensen, O., van den Brink, D., Weder, N., Schoffelen, J.-M., Magyari, L., Hagoort, P., & Bastiaansen, M. (2012). Beta oscillations relate to the N400m during language comprehension. *Human Brain Mapping*, *33*(12), 2898–2912. https://doi.org/10.1002/hbm.21410

Wen, H., & Liu, Z. (2016). Separating fractal and oscillatory components in the power spectrum of neurophysiological signal. *Brain Topography*, *29*(1), 13–26. https://doi.org/10.1007/s10548-015-0448-0

Wright, P., Stamatakis, E. A., & Tyler, L. K. (2012). Differentiating hemispheric contributions to syntax and semantics in patients with left-hemisphere lesions. *Journal of Neuroscience*, *32*(24), 8149–8157. https://doi.org/10.1523/JNEUROSCI.0485-12.2012

Yilmaz, U. (2021). *The earth mover's distance*. MATLAB Central File Exchange. Retrieved March 11, 2021, from https://www.mathworks.com/matlabcentral/fileexchange/22962-the-earth-mover-s-distance

Youssofzadeh, V., Stout, J., Ustine, C., Gross, W. L., Conant, L. L., Humphries, C. J., Binder, J. R., & Raghavan, M. (2020). Mapping language from MEG beta power modulations during auditory and visual naming. *NeuroImage*, *220*, e117090. https://doi.org/10.1016/j.neuroimage.2020.117090

Yuan, H., Liu, T., Szarkowski, R., Rios, C., Ashe, J., & He, B. (2010). Negative covariation between task-related responses in alpha/beta-band activity and BOLD in human sensorimotor cortex: An EEG and fMRI study of motor imagery and movements. *NeuroImage*, *49*(3), 2596–2606. https://doi.org/10.1016/j.neuroimage.2009.10.028

How to cite this article: Cao, Y., Oostenveld, R., Alday, P. M., & Piai, V. (2022). Are alpha and beta oscillations spatially dissociated over the cortex in context-driven spoken-word production? *Psychophysiology*, 59, e13999. https://doi.org/10.1111/psyp.13999